94-0; **24** (isomer 3), 124605-15-8; **25**, 124604-95-1; **26**, 124604-96-2; *anti*-**27**, 124605-05-6; *anti*-**28**, 124605-06-7; *anti*-**29**, 124618-73-1; *anti*-**30**, 124618-74-2; *anti*-**30** (3-ol derivative), 124618-75-3; **31**, 124649-63-4; **32**, 124605-07-8; **33**, 124605-08-9; **34**, 124605-09-0; **41**, 56761-11-6; **42**, 124649-64-5; **43**, 124649-65-6; **44**, 124649-66-7; **45**, 124605-12-5; (*E*)-**46**, 124605-13-6; (*Z*)-**46**, 124605-14-7; CH_3COCH_3, 67-64-1; $CH_3CH_2COCH_3$, 78-93-3; $(CH_3)_2CHCOCH_3$, 563-80-4; $(CH_3)_3CCOCH_3$, 75-97-8.

Photodimerization of Cyclohexene and Methane by Decatungstate Anions: Molecular Orbital Theory

Mohamed K. Awad and Alfred B. Anderson*

Contribution from the Chemistry Department, Case Western Reserve University, Cleveland, Ohio 44106. *Received February 13, 1989*

Abstract: A molecular orbital study has been made of the photodimerization of cyclohexene by excited $W_{10}O_{32}^{4-}$, yielding 3,3'-dicyclohexene to explain the observations of Yamase. The overall process is radical monomer coupling. Radical formation by an adiabatic H transfer from cyclohexene to O^- on the O 2p to W 5d charge transfer photoexcited oxyanion is described. This process is highly activated, just as on metal oxide surfaces, because of the stability which comes when an electron from the CH bond reduces the hole in the oxyanion O 2p band during H abstraction. Since α-H abstraction is stabilized by the formation of the allylic π orbital, the product selectivity can be understood. Calculated H abstraction activation energies for olefinic, α, and β CH bonds in cyclohexene and for a CH bond in CH_4 are higher, but they are low enough that in the case of CH_4 it can be suggested that dimerization could be looked for in future experiments using photoactivated oxyanions. Based on the calculated electronic structures, it is possible to envision a nonadiabatic electron transfer to O^- during mild thermal collisions between a CH bond and the clusters yielding an organic radical cation followed by proton transfer at a later time. Polar solvents would enhance the probability for this mechanism.

In the last decade, photoredox reactions involving polyoxometalates or polyoxoanions have received increased attention because of their high selectivity as reagents or catalysts for the photooxidation of organic substances.[1-7] These materials are stable for a number of photocatalytic oxidation reactions upon exposure to visible or near-ultraviolet light. Photocatalytic processes involving polyoxometalates and organic substrates lead in general to the reduction of the polyoxometalates and the oxidation of the organic substrates.

The light absorption step involves electron transfer from O^{2-} to the cation set of empty orbitals, forming the excited polyoxometalate $(P^{n-})^*$. This species reacts with the hydrocarbon R-H to form radicals R• which dimerize. There are two likely mechanisms for the formation of R•. The first is H abstraction by $(P^{n-})^*$:

$$(P^{n-})^* + RH \rightarrow PH^{n-} + R^\bullet \qquad (1)$$

and the second is electron transfer from R-H to $(P^{n-})^*$ followed by proton addition:

$$\begin{aligned}(P^{n-})^* + RH &\rightarrow P^{(n+1)-} + RH^{\bullet+} \\ &\rightarrow P^{(n+1)-} + R^\bullet + H^+ \\ &\rightarrow PH^{n-} + R^\bullet \end{aligned} \qquad (2)$$

As has been discussed,[8,9] the operative mechanism may be different for different systems. Hydride and proton elimination are unlikely first steps to R• formation.[3]

Yamase and co-workers studied the photocatalytic dimerization of olefins in acetonitrile by tetrakis(tetrabutylammonium)-decatungstate(VI), $[NBu_4]_4[W_{10}O_{32}]$.[10] Accompanying dimer formation was the reduction of the decatungstate by H atoms. The photocatalytic dimerization of cyclohexene by $[W_{10}O_{32}]^{4-}$ led to the formation of 3,3'-dicyclohexene as the main product of the oxidation process. Many other molecules were studied, and when dimerization was not observed, it was because of preferential dehydrogenation of OH groups present in the molecules to form aldehydes or in some cases, because of steric hindrance. Typical examples of these two effects were benzyl alcohol and norbornadiene.[10]

The formation of O^- hole centers on metal oxide surfaces is known to facilitate the dimerization of hydrocarbons by H abstraction followed by radical coupling.[11-13] The active O^- sites have been prepared by different methods, including charge-transfer excitation from O^{2-} to the empty cation band, γ-irradiation defect formation, cation doping, and chemical reactions. Molecular orbital theory has explained this activity in terms of the reduction of surface O^- by an electron from the CH bond during H atom abstraction.[14-17] The O^- prevents the high initial closed-shell

(1) Akid, R.; Darwent, J. R. *J. Chem. Soc., Dalton Trans.* **1985**, 395. Ioannidis, A.; Papaconstantinou, E. *Inorg. Chem.* **1985**, *24*, 439. Savinov, E. N.; Saidkhanov, S. S.; Parmon, V. N.; Zamaraev, K. I. *Dokl. Akad. Nauk. SSSR* **1983**, *269*, 1.
(2) Hill, C. L.; Bouchard, D. A. *J. Am. Chem. Soc.* **1985**, *107*, 5148.
(3) Renneke, R. F.; Hill, C. L. *J. Am. Chem. Soc.* **1988**, *110*, 5461.
(4) Hill, C. L.; Bouchard, D. A.; Kadkhodayan, M.; Williamson, M. M.; Schmidt, J. A.; Hilinski, E. F. *J. Am. Chem. Soc.* **1988**, *110*, 5471.
(5) Renneke, R. F.; Hill, C. L. *J. Am. Chem. Soc.* **1986**, *108*, 3528.
(6) Yamase, T.; Watanobe, R. *J. Chem. Soc., Dalton Trans.* **1986**, 1669.
(7) Yamase, T. *Polyhedron* **1986**, *5*, 79.
(8) Smegal, J. A.; Hill, C. L. *J. Am. Chem. Soc.* **1983**, *105*, 3515.
(9) Nappa, N.; Tolman, C. A. *Inorg. Chem.* **1985**, *24*, 4711.
(10) Yamase, T.; Usami, T. *J. Chem. Soc., Dalton Trans.* **1988**, 183.
(11) Kaliaguine, S. L.; Shelimov, B. N.; Kazansky, V. B. *J. Catal.* **1978**, *55*, 384.
(12) Driscoll, D. J.; Martir, W.; Wang, J.-X.; Lunsford, J. H. *J. Am. Chem. Soc.* **1985**, *107*, 58.
(13) Driscoll, D. J.; Lunsford, J. H. *J. Phys. Chem.* **1985**, *89*, 4415.
(14) Anderson, A. B.; Ray, N. K. *J. Am. Chem. Soc.* **1985**, *107*, 253.
(15) Mehandru, S. P.; Anderson, A. B.; Brazdil, J. F.; Grasselli, R. K. *J. Phys. Chem.* **1987**, *91*, 2930.
(16) Ward, M. D.; Brazdil, J. F.; Mehandru, S. P.; Anderson, A. B. *J. Phys. Chem.* **1987**, *91*, 6515.
(17) Mehandru, S. P.; Anderson, A. B.; Brazdil, J. F. *J. Am. Chem. Soc.* **1988**, *110*, 1715.

0002-7863/90/1512-1603$02.50/0

Table I[a]

atom	s			p			d					
	n	IP	ζ	n	IP	ζ	n	IP	ζ_1	c_1	ζ_2	c_2
C	2	15.09	1.658	2	9.76	1.618						
O	2	26.98	1.946	2	12.12	1.927						
H	1	12.1	1.20									
W	6	9.50	2.641	6	7.096	2.341	5	10.50	4.982	0.6940	2.068	0.5631

[a] Atomic parameters used in the calculations; principal quantum numbers, n, IP (eV), orbital exponents, ζ (au), and respectively linear coefficients, c, for double-ζ, d orbitals.

Table II. Calculated Diatomic Properties by Using the Atomic Parameters Given in Table I[a]

property	O–H	H_3C–H	W–O
D_e	4.50 (4.62[b,c])	5.34 (4.56[c,d])	7.86 (6.87[d,e])
R_e	1.09 (0.97[b])	1.21 (1.10[d])	1.77

[a] Dissociation energies, D_e (eV), and equilibrium bond lengths, R_e (Å). [b] Rosen, B. *Spectroscopy Data Relative to Diatomic Molecules*; Pergamon: Oxford, 1970. [c] D_0 value. [d] *CRC Handbook of Chemistry and Physics*; Weast, R. C., Ed.; CRC Press: Boca Raton, FL, 1986. [e] Huber, K. P.; Herzberg, G. Molecular Spectra and Molecular Structure IV. *Constants of Diatomic Molecules*; Van Nostrand: New York, 1979.

repulsion between CH and O during abstraction of H by O^{2-}. Further, the metal is already reduced, so the formation of an alkyl radical by O^- does not require promoting an electron over the gap to the oxide conduction band.

In this paper molecular orbital theory is used to examine the CH photoactivation mechanism for cyclohexene and methane by the $W_{10}O_{32}^{4-}$ anion of ref 10. The orbital interactions leading to a low activation energy for H transfer by reaction 1 are found, and the possibility of electron transfer being the first step in accordance with reaction 2 is discussed.

Theoretical Method

The atom superposition and electron delocalization molecular orbital (ASED-MO) theory[18] is employed. This is a semiempirical theoretical approach based on partitioning the electronic charge density into free atom parts and a component due to electron delocalization bond formation. As the atoms are brought into a molecular configuration, the electrostatic forces on one nucleus of each pair are integrated by using the electrostatic theorem to yield a repulsive energy due to rigid atom densities and an attractive energy due to electron delocalization. The sum is, without approximation, the molecular binding energy. In the ASED-MO method, the atom superposition energy is calculated by using atomic densities, and the electron delocalization energy is approximated by a one electron molecular orbital binding energy obtained by using a modified extended Hückel hamiltonian. The ASED-MO technique was used in the above-mentioned studies of CH bond activation by O^-[14-17] as well as by other oxide[19,20] and metal[21] surfaces. The atomic parameters used for W, O, C, and H in all calculations in this paper are in Table I. The oxygen anion 2s and 2p Slater exponents are decreased by 0.3 au from the atomic values of Clementi and Raimondi,[22] as was done for MoO_3 in ref 15. Because of ionicity, the ionization potentials for W are increased by 1.5 eV and for oxygen they are decreased by the same amount from the atomic values,[23] so that the charge transfer in diatomic WO is close to that deduced from Pauling's ionicity relationship. These shifts were also used for MoO_3.[15] The resulting predicted WO bond length is 1.77 Å. The diatomic W–O bond length is not known. The Slater exponents for C and H are the same as used in previous methane activation studies, e.g. ref 15, and their ionization potentials are decreased by 1.5 eV, as for oxygen. In all reported results for equilibrium structures, the bond lengths are variationally optimized to the nearest 0.1 Å and the bond angles to the nearest degree. Calculated bond energies and lengths for relevant single bonds are in Table II. The calculations typically overestimate CH bond lengths by about 0.1 Å.

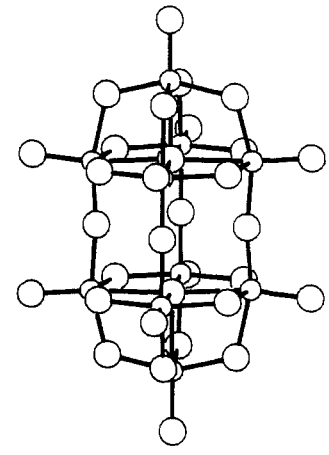

Figure 1. Structure of $W_{10}O_{32}^{4-}$. Smaller circles are W and larger ones are O.

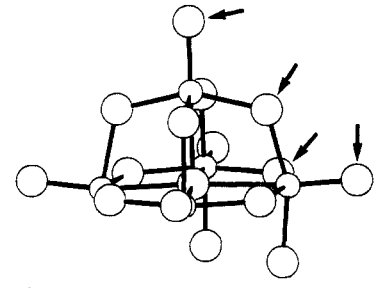

Figure 2. $W_5O_{16}^{2-}$ cluster model. The arrows indicate adsorption sites studied.

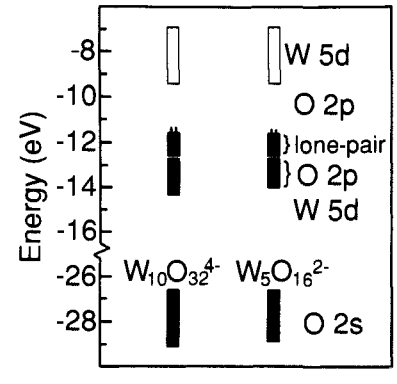

Figure 3. Electronic structure calculated for $W_{10}O_{32}^{4-}$ and $W_5O_{16}^{2-}$ model.

The decatungstate anion $[W_{10}O_{32}]^{4-}$ consists of two W_5O_{16} units, each is composed of five distorted WO_6 octahedra sharing edges and corners.[24] There are three types of W–O bonding configurations in the tungstate anion, with terminal, bridging, and central oxygen anions (Figure 1). There are two sets of terminal and bridging O^{2-}. The central O^{2-} has five

(18) (a) Anderson, A. B. *J. Chem. Phys.* **1975**, *62*, 1187. (b) Anderson, A. B.; Grimes, R. W.; Hong, S. Y. *J. Phys. Chem.* **1987**, *91*, 4245.
(19) Anderson, A. B.; Ewing, D. W.; Kim, Y.; Grasselli, R. K.; Burrington, J. D.; Brazdil, J. F. *J. Catal.* **1985**, *96*, 222.
(20) Mehandru, S. P.; Anderson, A. B.; Brazdil, J. F. *J. Chem. Soc., Faraday Trans. 1* **1987**, *83*, 463.
(21) Anderson, A. B.; Kang, D. B.; Kim, Y. *J. Am. Chem. Soc.* **1984**, *106*, 6597. Mehandru, S. P.; Anderson, A. B. *J. Am. Chem. Soc.* **1985**, *107*, 844. Kang, D. B.; Anderson, A. B. *J. Am. Chem. Soc.* **1985**, *107*, 7858. Kang, D. B.; Anderson, A. B. *Surf. Sci.* **1986**, *165*, 221. Kang, D. B.; Anderson, A. B. *Surf. Sci.* **1985**, *155*, 639. Anderson, A. B.; Maloney, J. J. *J. Phys. Chem.* **1988**, *92*, 809.
(22) Clementi, E.; Raimondi, D. L. *J. Chem. Phys.* **1963**, *38*, 2686 (for first two rows of periodic table).
(23) Lotz, W. *J. Opt. Soc. Am.* **1970**, *60*, 206.
(24) Sasaki, Y.; Yamase, T.; Chashi, Y.; Sasada, Y. *Bull. Chem. Soc. Jpn.* **1987**, *60*, 4285.

Table III. Calculated OH Bond Lengths, R_e (Å) and Dissociation Energies D_e (eV) for H Bound to $(W_5O_{16}^{2-})^*$ Cluster

bond property	site: equatorial terminal	equatorial bridging	capped terminal	capped bridging	central
R_e	1.09	1.09	1.09	1.08	1.07
D_e	5.15	4.93	5.13	4.83	4.46

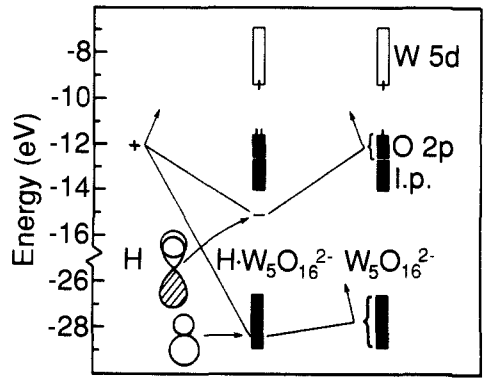

Figure 4. Correlation diagram for H binding to an O^-.

bonds with the surrounding W cations. The ^{183}W NMR spectrum showed that there are two types of W(VI), eight equatorial and two capped in the $[W_{10}O_{32}]^{4-}$ structure.[10] A $[W_5O_{16}]^{2-}$ cluster (Figure 2), which is exactly the half-moiety of $[W_{10}O_{32}]^{4-}$, is used as a cluster model in the CH activation studies. Experimentally,[24] in the $[W_5O_{16}]^{2-}$ cluster one of the bridging W–O bond lengths is 1.89 Å and one of the terminal bonds is 1.74 Å. Using the above parameters and experimental positions for all of the other atoms in the cluster, the calculations yield 1.93 and 1.79 Å, respectively. While a slight increase in oxygen exponents would allow matching these distances to 0.01 Å, such changes would be ad hoc and would provide no further insight in the following, so they are omitted. The energy levels for this model and the decatungstate anion $[W_{10}O_{32}]^{4-}$ are essentially the same, as shown in Figure 3. The calculated electronic structure has four parts. The lowest two bands comprise W–O bonding orbitals of predominately O 2s and O 2p character and are filled. The third band is also filled and corresponds to O 2p dangling lone-pair orbitals. The antibonding counterparts are localized predominately on W and are empty because W is in the +6 oxidation state. The electronic spectra of $[W_{10}O_{32}]^{4-}$ in acetonitrile show an absorption maximum at 323 nm due to O → W charge transfer. The band edge is ~435 nm. The calculated band gap between the top of 2p dangling orbitals and the bottom of the W band is 2.2 eV, which is in satisfactory agreement with the observed band edge at 2.8 eV. According to experimental results,[25-27] nonplanar cyclohexene is most stable in the half-chair conformation, with C_2 symmetry. This structure, with data from ref 27, is used in the calculations.

Results and Discussion

The binding of H to the charge-transfer excited cluster with a delocalized hole in the O 2p band is examined first. The hydrogen could adsorb at different oxygen sites in the $[W_5O_{16}]^{2-}$ cluster shown by arrows in Figure 2. The calculations predict that it binds to terminal oxygens more strongly than to bridging and central ones. In each case a σ bond is formed as shown in Figure 4. These results are summarized in Table III. The hydrogen binds most strongly to the equatorial terminal oxygen atoms. This agrees with the ESR results for hydrogenation of $[W_{10}O_{32}]^{4-}$, which showed that water molecules donate hydrogen to the terminal oxygen atoms at the equatorial WO_6 sites.[10]

Methane activation was studied on the same excited-state cluster. The H-abstraction transition states are reached when the CH bond is stretched by 0.03 Å toward a bridging oxygen and 0.14 Å toward a terminal one; the respective OH distances are 1.56 and 1.40 Å. The activation barriers are 0.75 eV in the first case and 0.51 eV in the second. These barriers are similar to those of the earlier theoretical study of CH_4 activation by O^- on MoO_3 (0.7 eV).[15] The structure of the transition state at the terminal site may be seen in Figure 5. Figure 6 shows the orbital correlations at the transition state. The electron-hole transfers to the antibonding CH–O level as soon as it reaches the top of the O 2p band, and the transition state is reached with a slight additional CH stretch. The photoexcitation of an electron lowers the repulsion that occurs on the initial approach by increasing the bond order between H and O. The activation energy is low because an electron from the CH bond need only be promoted to the hole level, and not to the metal. OH^- and $CH_3^\bullet$ are formed:

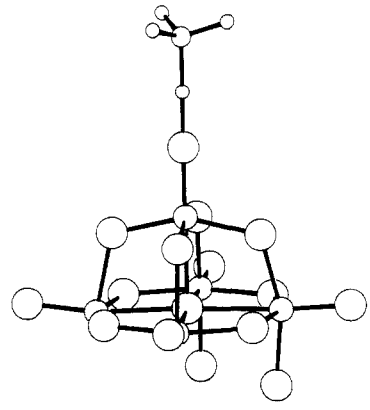

Figure 5. Transition state for H transfer from methane to a terminal O^-.

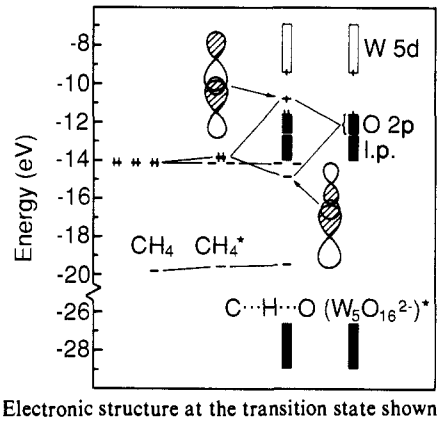

Figure 6. Electronic structure at the transition state shown in Figure 5. The second column of levels (CH_4^*) shows how a σ orbital is destabilized on stretching to the transition state in the absence of the cluster.

$$W^{V}O^- + CH_4 \rightarrow W^{V}OH^- + CH_3^\bullet \quad (3)$$

If the $CH_3^\bullet$ generated from the activation of CH_4 by O^- binds to the cluster, it is formally oxidized to CH_3^+ and a second electron is added to the W 5d band. The calculated binding energy for $CH_3^\bullet$ on a terminal O^{2-} is only 0.14 eV, so it will not stick to the cluster at room temperature. This means that two $CH_3^\bullet$ can combine and form ethane:

$$2CH_3^\bullet \rightarrow C_2H_6 \quad (4)$$

This is exactly what happens experimentally over MgO when O^- is present;[12] in this case $CH_3^\bullet$ is predicted to desorb.[17] With the calculated hydrogen atom binding energies at different sites, the $CH_3^\bullet$ forming reactions are uphill for bridging and terminal oxygen sites by 0.51 and 0.21 eV, respectively, which are both less than the calculated activation energies of 0.75 and 0.51 eV.

Similar calculations of the activation of cyclohexene by O^- on the $[W_5O_{16}]^{2-}$ cluster model were performed. Optimized C–H bond lengths for the olefinic, α, and β hydrogens of cyclohexene were used. In the case of olefinic H abstraction by the terminal oxygen of the $[W_5O_{16}]^{2-}$ cluster, the activation barrier is 0.49 eV, and smaller barriers are found for α and β hydrogen, 0.14 and 0.29 eV, respectively. Figure 7 shows the structure of the transition state for α-H abstraction; the CH bond is stretched by 0.17 Å

(25) Scharpen, L. H.; Wollrab, J. E.; Ames, D. P. *J. Chem. Phys.* **1968**, *49*, 2368.
(26) Naumov, V. A.; Bezzubov, V. M. *J. Struct. Chem. (Engl. Transl.)* **1967**, *8*, 466.
(27) Chiang, J. F.; Bauer, S. H. *J. Am. Chem. Soc.* **1969**, *91*, 1898.

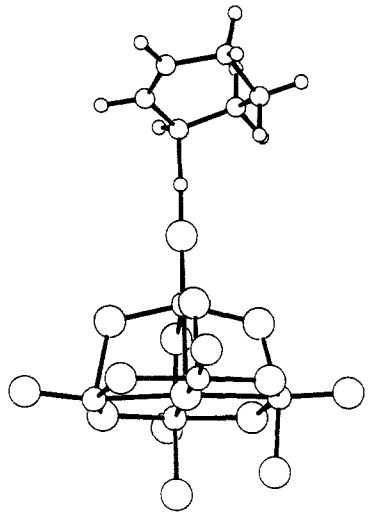

Figure 7. Transition state for H transfer from cyclohexene to a terminal O^-.

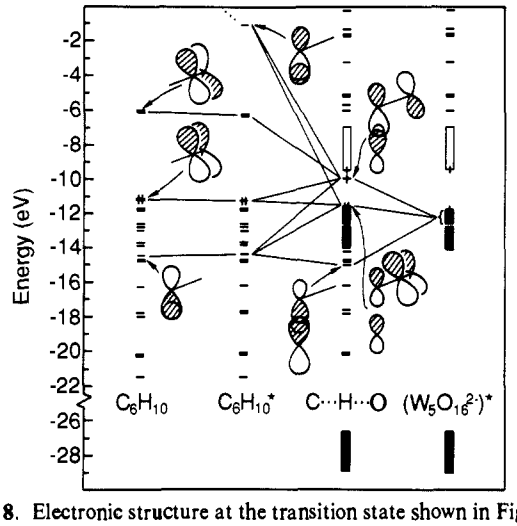

Figure 8. Electronic structure at the transition state shown in Figure 7. The C_6H_{10}* column shows energy levels in transition-state structure with cluster absent.

and the O–H distance is 1.40 Å. The transition state for olefinic H abstraction is reached when the OH distance is 1.40 Å and the CH bond is stretched 0.10 Å. The low 0.14 eV activation energy for this H abstraction is of particular interest. The out-of-plane α-CH bonds in propylene are known to be especially weak because when these bonds are stretched a p orbital component on the α-C is freed up to mix with and stabilize the adjacent π orbital.[28] In cyclohexene both α-H on each α-C are out-of-plane. A comparison of the electronic structure on going to the transition state for α-H abstraction in Figure 8 with that for CH_4 in Figure 6 shows the same σ donation with antibonding counterpart interaction at the transition states. The above-mentioned π stabilization is clearly evident at the α-H abstraction transition state in Figure 8. Because of hybridization of the empty CH σ^*, which has been significantly stabilized by the 0.17 Å CH bond stretch, the 1s contribution on H is negligible so that the CH interaction with O in this orbital is close to nonbonding instead of being strongly antibonding. Indeed, the stabilization of the π orbital for the transition state is calculated to be 0.34 eV, which is the same as 0.3 eV calculated for removal of an out-of-plane α-H when keeping the propylene framework rigid as calculated in ref 28. This means the π orbital stabilization is essentially complete at the transition state, and this is the cause of the low barrier for α-H abstraction. The combination of two C_6H_9* formed by α-hydrogen abstraction explains the observation of 3,3′-dicyclohexene as the product observed[10] for photodimerization:

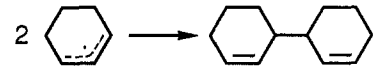

The discussion so far has focused on the adiabatic energy surface and transition-state electronic structure for CH activation and H atom transfer to O^-. The possibility of electron transfer and the formation of radical cations is suggested by Figures 6 and 8, where it may be seen that the O^- hole at the top of the O 2p valence band appears to be reduced even before the transition state is reached. Of course this is not exactly what is happening since the CH σ–O 2p antibonding counterpart orbital is occupied by one electron, but this is the orbital that ultimately becomes the radical orbital on C. The charge delocalization from the hydrocarbon molecule to the cluster is becoming substantial at the transition state, 0.33 electron for CH_4 and 0.47 electron for C_6H_{10} in the case of α-H abstraction, according to Mulliken partitioning. The corresponding charges on the transferring H atoms are 0.16 and 0.17 electron charge unit. One could say, then, that to the extent of these charge magnitudes, at the transition state the electron transfer is ca. $^1/_3$ to $^1/_2$ complete. This description fits the concerted electron plus proton process of eq 1, however, and not the sequential one of eq 2. For the latter process a nonadiabatic collision between H and O^- must be envisioned. It would not take much thermal collision energy for the CH bond electron pair to interact with an O lone pair strongly enough to raise the antibonding counterpart orbital energy level to the top of the O 2p band. The O^- hole is delocalized and this is the factor that might allow the nonadiabatic transfer of an electron to the cluster during the collision. Polar solvents, such as commonly used acetonitrile, would assist by providing shielding of the electrostatic interactions between the radical cation and the cluster and by solvating the radical cation. The fact that it is the weakest (α-CH) bond that is broken in cyclohexene dimerization is necessary but not sufficient for proving the H-abstraction mechanism of eq 1. Interactions that would favor radical cation formation would also stabilize other ionic intermediates. For example, R* might bond to O^{2-}, reducing the oxyanion cluster and with sufficient electron delocalization and solvent stabilization R^+ could depart from the cluster as a solvated cation. Reduction of R* to R^- could also be envisioned. The experimental evidence seems to not favor the formation of carbonium and carbanion intermediates.[3]

Conclusions

From this theoretical study it is concluded that the processes of radical formation and their dimerization over photoactivated decatungstate anions,[10] and probably over polyoxometalates[29] in general, are the same as on metal oxide surfaces having a nonadiabatic electron transfer. H abstraction from a CH bond is activated by the stability that comes from reducing an O 2p hole in the charge-transfer photoactivated polyoxometalate. This electron comes from the CH bond being promoted to the O 2p hole orbital by a slight CH bond stretch to the transition state. The lowest CH activation energy for cyclohexene is for the out-of-plane α-CH bonds, a result of π-orbital stabilization attendant to stretching these CH bonds. This explains the selectivity for 3,3′-dicyclohexene. By analogy with known oxide surface chemistry, the selective oxidation and dimerization of CH_4 may be possible over photoactivated polyoxometalates. The possibility of nonadiabatic electron transfer from hydrocarbon molecules to O^- on photoexcited polyoxyanions cannot be ruled out. Strongly polar solvents would favor this. Proton transfer would follow at a later time according to eq 2.

Acknowledgment. M.K.A. is grateful for a fellowship from the Government of Egypt during his leave of absence from Tanta University. We also thank the Gas Research Institute for support, and express our appreciation to a reviewer for insightful comments.

(28) Fang, H. L.; Swofford, P. L.; McDevitt, M.; Anderson, A. B. *J. Phys. Chem.* **1985**, *89*, 225.

(29) Yamase, T. *J. Chem. Soc., Dalton Trans.* **1985**, 2585.